The Journal of Immunology

Microsomal Prostaglandin E Synthase-1 Is a Major Terminal Synthase That Is Selectively Up-Regulated During Cyclooxygenase-2-Dependent Prostaglandin E_2 Production in the Rat Adjuvant-Induced Arthritis Model

David Claveau, Mirna Sirinyan, Jocelyne Guay, Robert Gordon, Chi-Chung Chan, Yves Bureau, Denis Riendeau and Joseph A. Mancini

J Immunol 2003; 170:4738-4744; ;
doi: 10.4049/jimmunol.170.9.4738
http://www.jimmunol.org/content/170/9/4738

The Journal of Immunology is published twice each month by
The American Association of Immunologists, Inc.,
1451 Rockville Pike, Suite 650, Rockville, MD 20852

Print ISSN: 0022-1767 Online ISSN: 1550-6606.

Microsomal Prostaglandin E Synthase-1 Is a Major Terminal Synthase That Is Selectively Up-Regulated During Cyclooxygenase-2-Dependent Prostaglandin E_2 Production in the Rat Adjuvant-Induced Arthritis Model

David Claveau,[1]* Mirna Sirinyan,[1‡] Jocelyne Guay,* Robert Gordon,[†] Chi-Chung Chan,[†] Yves Bureau,[†] Denis Riendeau,* and Joseph A. Mancini[2]*

To better define the role of the various prostanoid synthases in the adjuvant-induced arthritis (AIA) model, we have determined the temporal expression of the inducible PGE synthase (mPGES-1), mPGES-2, the cytosolic PGES (cPGES/p23), and prostacyclin synthase, and compared with that of cyclooxygenase-1 (COX-1) and COX-2. The profile of induction of mPGES-1 (50- to 80-fold) in the primary paw was similar to that of COX-2 by both RNA and protein analysis. Quantitative PCR analysis indicated that induction of mPGES-1 at day 15 was within 2-fold that of COX-2. Increased PGES activity was measurable in membrane preparations of inflamed paws, and the activity was inhibitable by MK-886 to ≥90% with a potency similar to that of recombinant rat mPGES-1 (IC_{50} = 2.4 μM). The RNA of the newly described mPGES-2 decreased by 2- to 3-fold in primary paws between days 1 and 15 postadjuvant. The cPGES/p23 and COX-1 were induced during AIA, but at much lower levels (2- to 6-fold) than mPGES-1, with the peak of cPGES/p23 expression occurring later than that of COX-2 and PGE_2 production. Prostacyclin (measured as 6-keto-$PGF_{1\alpha}$) was transiently elevated on day 1, and prostacyclin synthase was down-regulated at the RNA level after day 3, suggesting a diminished role of prostacyclin during the maintenance of chronic inflammation in the rat AIA. These results show that mPGES-1 is up-regulated throughout the development of AIA and suggest that it plays a major role in the elevated production of PGE_2 in this model. ***The Journal of Immunology*, 2003, 170: 4738–4744.**

Prostaglandins are potent lipid mediators formed during pain and inflammation that are derived through the enzyme-catalyzed conversion of arachidonic acid by cyclooxygenase (1). Studies with deletion of the PG receptors and a neutralizing mAb to PGE_2 have demonstrated that PGE_2 and PGI_2 are the primary prostanoids involved in inflammation and inflammatory pain responses (1, 2). The clinical development and efficacy of cyclooxygenase-2 (COX-2)[3] inhibitors have demonstrated that this is the major form of cyclooxygenase involved in prostanoid synthesis during pain and inflammatory responses (3). The recent identification of several PGE synthases (PGES) has led to the proposal that specific terminal synthases may play different roles in PGE_2 formation (4–6). The inducible PGES (mPGES-1) has been shown to be up-regulated during LPS-induced pyresis and in the presence of IL-1β, and also down-regulated by dexamethasone (7, 8). A cytosolic PGES (cPGES/p23) has been demonstrated to couple more efficiently with COX-1 as compared with COX-2 (5). There are also several other proteins with PGES activity, including two μ class glutathione transferases (9) and a recently identified mPGES-2 (10). The two μ class glutathione transferases with PGES activity have high K_{ms} for PGH_2 and relatively low specific activities. The mPGES-2 enzyme is expressed constitutively in many tissues, including brain, heart, skeletal muscle, kidney, and liver, and has not been characterized for regulation of expression.

PGE_2 also plays a major physiological role in tissues, such as in the kidney, where it is involved in maintaining sodium homeostasis (11). Immunohistochemical analysis has localized mPGES-1 to epithelia of distal tubules and medullary-collecting ducts in the mouse kidney (12). The renal localization of mPGES-1 overlaps with both COX-1 and COX-2 expression and suggests that coupling of mPGES-1 with either COX enzyme may be possible depending on the tissue. The inducible synthase (mPGES-1) has also been demonstrated to be colocalized with COX-2 in brain-derived endothelial cells upon IL-1β stimulation (8, 13). This suggests a role for mPGES-1 in pyresis because COX-2-derived PGE_2 acting through the EP3 receptor has been delineated as the mechanism of induction of pyresis (14–16). Furthermore, mPGES-1 has been shown to be colocalized with COX-2 in mouse peritoneal macrophages stimulated with LPS (17). A recent study has demonstrated that LPS-induced PGE_2 production in peritoneal macrophages from mPGES-1 null mice is abolished, suggesting that mPGES-1 plays a significant role in PGE_2 generation under inflammatory conditions (18). A model of chronic joint inflammation in which PGs play a significant role is the adjuvant-induced arthritis (AIA) in rats (19, 20). We have performed a detailed time course analysis in this model comparing the expression of mPGES-1, mPGES-2,

*Departments of Biochemistry and Molecular Biology and [†]Pharmacology, Merck Frosst Center for Therapeutic Research, Kirkland, Quebec, Canada; and [‡]Department of Pharmacology and Experimental Therapeutics, McGill University, Montreal, Quebec, Canada

Received for publication September 11, 2002. Accepted for publication February 24, 2003.

The costs of publication of this article were defrayed in part by the payment of page charges. This article must therefore be hereby marked *advertisement* in accordance with 18 U.S.C. Section 1734 solely to indicate this fact.

[1] D.C. and M.S. contributed equally to this manuscript.

[2] Address correspondence and reprint requests to Dr. Joseph A. Mancini, Merck Frosst Center for Therapeutic Research, PO Box 1005, Pointe-Claire-Dorval, Quebec, H9R 4P8. E-mail address: joseph_mancini@merck.com

[3] Abbreviations used in this paper: COX, cyclooxygenase; AIA, adjuvant-induced arthritis; PGES, PGE synthase; cPGES, cytosolic PGES; mPGES, membrane PGES; PGIS, prostacyclin synthase; PVDF, polyvinylidene difluoride.

0022-1767/03/$02.00

and cPGES/p23 in relationship with paw edema formation, COX-2 and COX-1 expression, and PGE_2 production.

Materials and Methods

AIA model

All procedures used in the in vivo assays were approved by the Animal Care Committee at the Merck Frosst Center for Therapeutic Research (Kirkland, Quebec, Canada), according to guidelines established by the Canadian Council on Animal Care.

The AIA model was performed with Harlan Sprague Dawley (Indianapolis, IN) rats. Animals were anesthetized with a ketamine/xylazine injection i.m., before an intradermal injection of 0.5 mg of *Mycobacterium butyricum* in mineral oil that was administered into the right hind footpad, as described previously (21). Paw volumes were determined using a water plethysmometer (Ugo Basile, Varese, Italy) at the indicated points in the time course. Rats were euthanized by carbon dioxide inhalation. The tissues were flash frozen in liquid nitrogen.

Total RNA isolation and reverse transcription

Frozen paws were pulverized with a mortar and pestle and dissolved in TRIzol reagent (Canadian Life Technologies, Burlington, Ontario, Canada). Total RNA was isolated using TRIzol reagent, according to the manufacturer's instructions. After dissolving the RNA, an equal volume of RNAmate (BioChain Institute, Hayward, CA) was added to precipitate the RNA and eliminate potential polysaccharides and proteoglycan contamination. A cleanup of the RNA was then performed using the Rneasy mini kit (Qiagen, Chatsworth, CA), as described in the manufacturer's instructions. Reverse transcription of RNA (50 ng) was performed using Taqman transcription reagents (PE Biosystems, Foster City, CA). The reaction was performed in the presence of 1× TaqMan reverse-transcription buffer, 5.5 mM magnesium chloride, 500 μM each dNTP, 2.5 μM random hexamers, 0.4 U/μl RNase inhibitor, and 1.25 U/μl Multiscribe reverse transcriptase. Every reaction set included RNA samples incubated in the absence of Multiscribe reverse transcriptase to serve as controls for genomic DNA contamination. The cycling parameters consisted of a primer incubation of 10 min at 25°C, reverse transcription for 30 min at 48°C, followed by inactivation at 95°C for 5 min.

Real-time quantitative PCR

PCR primers and TaqMan hydrolysis probes for all target genes except the 18S ribosomal RNA (18S rRNA) were designed using the Primer Express software (PE Biosystems, Foster City, CA) and synthesized at Integrated DNA Technologies (Coralville, IA) (Table I). The rat mPGES-2 partial sequence was obtained by sequencing of a rat expressed sequence tag (GenBank BF558739). The sequences of the primers used are presented in Table I. Predeveloped 18S rRNA primers and probe set were purchased from PE Biosystems. All Taqman hydrolysis probes except the 18S rRNA probe consisted of a gene-specific oligonucleotide dually labeled with a 6-FAM reporter dye at the 5′ end and a Black Hole Quencher-1 quencher dye at the 3′ end. The 18S rRNA probes differed in that they contained a VIC reporter dye at the 5′ end and a TAMRA quencher dye at the 3′ end. Primer specificity of amplification was confirmed by gel electrophoresis. Real-time PCR was performed on an ABI Prism 7700 Sequence Detection System (PE Biosystems). Each PCR, except for the 18S rRNA, was performed in a total volume of 50 μl, containing 5 μl cDNA, 25 μl TaqMan Universal PCR Master Mix (PE Biosystems), 900 nM forward and reverse primers, 300 nM TaqMan probe, and nuclease-free water (Ambion, Austin, TX) to complete. PCR for the 18S rRNA were performed in a similar way, except that 2.5 μl of the commercial primers/probe set was used. The cycling parameters consisted of 2-min uracil removal incubation at 50°C, 10-min polymerase activation at 95°C, 50 cycles of denaturation at 95°C for 15 s, and annealing/extension at 60°C for 1 min. Every reaction set included a reaction in which water was used instead of cDNA to serve as a control for DNA contamination and probe degradation.

Statistical analysis of data

The quantitative PCR analysis presented in Fig. 2 was analyzed by both a paired *t* test and 2 × 10 mixed (split-plot) ANOVA design. Because the adjuvant was administered to one rear paw (primary), whereas the other was used as a control (secondary), the treatment (adjuvant) variable was analyzed as a within-subjects factor. The time course variable in contrast was analyzed as a between-subjects factor. All analyses were conducted using SPSS (Chicago, IL) software, version 10. The induction of COX-2 mRNA expression was statistically significant and related to the adjuvant treatment (adjuvant main effect, $F(1, 18) = 66.93$, $p < 0.001$; time course main effect, $F(9, 18) = 3.21$, $p < 0.05$; interaction, $F(1, 9) = 3.61$, $p < 0.05$). The induction of mPGES-1 was also statistically significant for all three parameters (adjuvant main effect, $F(1, 18) = 109.35$, $p < 0.001$; time course main effect, ($F(9, 18) = 4.68$, $p < 0.01$; interaction, $F(9, 18) = 4.86$, $p < 0.01$). The analyses of mPGES-2 mRNA demonstrates a slight reduction of expression with adjuvant treatment that is statistically significant (adjuvant main effect, $F(1, 18) = 46.81$, $p < 0.001$; interaction, $F(9, 18) = 4.84$, $p < 0.01$). We have analyzed cPGES/p23 and COX-1 expression and found no statistically significant effect for cPGES/p23, while the 3- to 5-fold increase in COX-1 was statistically significant (cPGES/p23, adjuvant main effect, $F(1, 18) = 0.001$, p = NS; COX-1, adjuvant main effect, $F(1, 18) = 106.81$, $p < 0.001$; time course main effect, $F(9, 18) = 3.48$, $p < 0.05$; interaction, $F(9, 18) = 4.27$, $p < 0.01$).

Quantitation of gene expression

The quantification of the real-time PCR results was performed as described in User Bulletin 2 of the ABI Prism 7700 Sequence Detection System (PE Biosystems) using the relative standard curve method. Briefly, PCR for all samples were performed in parallel to standardization series made with known dilutions of the cDNA of the secondary paw of one animal at day 0 as template. Measured fluorescent signal intensities were plotted against the number of PCR cycles on a semilogarithmic scale. The cycle number in which the PCR amplification was in its exponential phase was compared with the standardization series values to obtain the relative quantity of the sample. To normalize for the amounts of RNA, PCR for the target genes and for the 18S rRNA endogenous reference were performed in separate tubes for each sample, and the target relative quantities were divided by the 18S rRNA quantities to obtain normalized target values. To obtain the relative expression level of each sample, the normalized target values of each sample are divided by the normalized target value of the control, which was chosen as the secondary paw of one animal at day 0. Absolute

Table I. *Primer and probe oligonucleotide sequences for real-time quantitative PCR*[a]

Gene	Accession No.	Primers	Probe
mPGES-1	AB041998	Forward: 5′-GCGAACTGGGCCAGAACA-3′ Reverse: 5′-GGCCTACCTGGGCAAAATG-3′	5′-CCCCGGAGCGAATGCGTGG-3′
COX-2	S67722	Forward: 5′-CATGATCTACCCTCCCCACG-3′ Reverse: 5′-CAGACCAAAGACTTCCTGCCC-3′	5′-CCTGAGCACCTGCGGTTCGCTG-3′
mPGES-2	—[b]	Forward: 5′-GGCAGTGGGCGGATGA-3′ Reverse: 5′-TCGGCAGGTGTTCGGTACA-3′	5′-TGGCTGGTGCATCTCATCTCTCCCA-3′
COX-1	S67721	Forward: 5′-TCCGTGAAGATGCGCTACC-3′ Reverse: 5′-AACACCTCCTGGGCCACAG-3′	5′-CCAGGTGTCCCGCCCGAAAAG-3′
cPGES	—[c]	Forward: 5′-TCCTGGCCTAGGTTAACAAAGG-3′ Reverse: 5′-CCTCCCAGTCTTTCCAATTATTGA-3′	5′-GTCCACACTAAGCCAATTAAGCTTTGCCCTT-3′
PGIS	NM_031557	Forward: 5′-GACGTTTTCCGCACCTTCC-3′ Reverse: 5′-ACTGACAAGGAGCCTCGAGC-3′	5′-CCAGCTGGATCTGATGCTCCCCA-3′

[a] All cDNA sequences except the cPGES and mPGES-2 sequence were obtained from the GenBank database. The Taqman hydrolysis probes are gene-specific oligonucleotides dually labeled with a 6-FAM reporter dye at the 5′ end and a Black Hole Quencher-1 quencher dye at the 3′ end.

[b] The partial cDNA sequence of rat mPGES-2 was obtained by PCR sequencing of rat expressed sequence tag GenBank BF558739.

[c] The cDNA sequences of the rat cPGES were kindly provided by L. Boulet at Merck Frosst.

quantification was performed using standard curves made from serial dilutions of known amounts of plasmids containing the cDNA of the genes of interest. PCR for the samples were performed in parallel with the standard curves, and the Ct (threshold cycle) values of the samples were compared with the standard curves values to obtain the mass amount of DNA. Then, using the m.w. of each cloned cDNA, respectively, to their vector, a conversion to a molar amount has been performed.

Protein preparation and immunoblot analysis

Frozen rat paws were pulverized using a mortar and pestle, resuspended in PBS (Invitrogen, San Diego, CA) with 2.6 mM DTT and 1× Complete Protease Inhibitor mixture (Roche, Mannheim, Germany), and sonicated three times for 30 s at 4°C using a Cole Parmer 4710 Ultrasonic Homogenizer. Disrupted paws were subjected to centrifugation at 1,000 × *g* for 10 min, and the supernatant was further centrifuged at 100,000 × *g* for 1.5 h. The membrane pellet was resuspended in PBS with 2.6 mM DTT and 1× Complete Protease Inhibitor mixture, and protein concentrations were determined using a Bio-Rad protein assay (Bio-Rad, Hercules, CA). Protein samples were resolved by SDS-PAGE using 4–20% gradient gels supplied by Novex (Invitrogen) and transferred electrophoretically to polyvinylidene difluoride (PVDF) membranes using a Novex immunoblot transfer apparatus, according to the manufacturer's instructions. Nonspecific sites on PVDF membranes were blocked with 5% nonfat dry milk in PBST for 1 h at room temperature, followed by two 5-min washes with PBST. The PVDF membrane was probed with either a 1/300 dilution of PGES antisera (Cayman Chemical, Ann Arbor, MI), or a 1/450 dilution of COX-2 antisera (Cayman Chemical), or a 1/1000 dilution of cPGES/p23 antisera (Affinity BioReagents, Golden, CO) in 1% milk/PBST for 1 h. The blot was washed once for 15 min with PBST, followed by four times for 5 min with PBST, and then incubated with a 1/3000 dilution of HRP-linked secondary Ab (Amersham Pharmacia Biotech, Piscataway, NJ) in 1% milk/PBST for 1 h. The washing steps were repeated, and subsequently, ECL detection was performed, according to the manufacturer's instructions (PerkinElmer Life Sciences, Wellesley, MA). Detection and quantitative analysis were performed using a Fuji Film LAS-1000 charge-coupled device and Image Gauge software.

PGES activity

The soluble fraction (100,000 × *g* supernatant) and microsomal membranes (100,000 × *g* pellet) prepared from the rat paws, as described above, were assayed for PGES activity (7). Samples were diluted into 0.1 M potassium phosphate, pH 7.0, 2 mM EDTA, and 2.5 mM reduced glutathione. The reaction was initiated with 1 μM PGH_2 and terminated after 40 s with 0.1 N HCl and 1 mg/ml stannous chloride. PGE_2 production was determined by enzyme immunoassay analysis, according to the manufacturer's instructions (Assay Designs, Ann Arbor, MI).

Results

Inflammatory response in paws during AIA

AIA in rats is a model of inflammation that has been demonstrated to contain a significant PG component through the induction of COX-2 and of PGE_2 synthesis. The present study was performed with SD rats injected with 0.5 mg of *M. butyricum* into the hind foot pad (primary paw), and the inflammatory response was followed over 25 days. During this time period, the paw volume increased from 1.5 ml on day 0 to a maximum of 5.0 ml by day 25 postadjuvant treatment in the primary paw (Fig. 1). The secondary paw (uninjected hind paw) also increased in volume, but at a much slower rate, with a maximum volume of 3.0 ml on day 25. Additional controls with rats treated with saline vehicle were analyzed on days 15 (15N) and 25 (25N) of the study (Fig. 1). The primary and secondary paws were collected and analyzed for RNA, protein expression, and PG production to examine the temporal expression of mPGES-1, mPGES-2, cPGES/p23, COX-1, COX-2, and prostacyclin synthase (PGIS).

RNA expression of the terminal synthases during AIA

The oligonucleotide sequences of Taqman primer probe sets used for the RNA analysis for mPGES-1, cPGES/p23, mPGES-2, COX-2, COX-1, and PGIS are described in Table I. RNA analyses were performed on samples from paws collected at different time

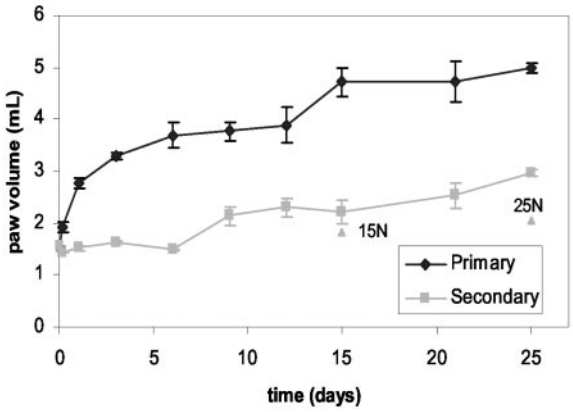

FIGURE 1. Time course of edema formation in the AIA model. Paw volumes were evaluated based on water displacement using a plethysmometer. The 15N and 25N samples are normal animals injected with a vehicle control for which paws were collected at days 15 and 25, respectively. The primary paw is injected with *M. butyricum*, and the secondary paw is from the same animal with no treatment. Results are expressed as mean ± SEM of paw volume (ml) for $n = 5$ rats.

points (Fig. 2) following adjuvant treatment, and were calculated as relative expression to the secondary paw at day 0 (18S ribosomal RNA was used to normalize the RNA levels from the various samples). The mPGES-1 RNA level was increased 49-fold by the 4-h time point in the primary paw following adjuvant administration. The induction of mPGES-1 was maximal during the first 3 days (50- to 76-fold), remained elevated during the progression of inflammation (20- to 40-fold up to day 15), and decreased over time to a 10-fold relative induction at day 25. This increase in expression was statistically significant throughout the time course (see all ANOVA analyses in *Materials and Methods*). COX-2 mRNA was also increased at 4 h, achieving a maximal relative induction of 92-fold within the first 3 days and decreasing at longer time points to 18- to 30-fold at days 21–25. In the secondary paws, lower levels of mPGES-1 and COX-2 were detected with a maximal induction of 3- to 4-fold. COX-1 RNA expression was not induced at the 4-h and 1-day time points, but showed a 3- to 5-fold induction from days 3–25 in the primary paw. The cPGES, which has been shown to preferentially couple with COX-1 (5) for the synthesis of PGE_2, also showed a slight induction at the RNA level (up to 2- to 3-fold) during the 25-day time course. There was no significant main effect for time course or time course by treatment interaction, indicating that treatment did not have a differential effect on cPGES/p23 RNA levels over time. The RNA expression of mPGES-2 was also analyzed over this time course, and mPGES-2 levels were decreased ~2-fold between days 1 and 12 and at day 21. The prostacyclin receptor knockout demonstrated that PGI_2 may play a role in an acute model of rodent inflammation (22). We analyzed PGIS RNA expression and observed a decrease of 3- to 9-fold in the primary paw from days 3 to 25.

We have also quantitated the amount of COX-1, COX-2, mPGES-1, and cPGES/p23 RNA transcripts using standard curves obtained with the same Taqman primers and corresponding cDNA fragments (Fig. 3). The quantitation indicates that at day 15, in the primary paw, the number of RNA transcripts of COX-2 exceeds those of COX-1 by ~10-fold. In addition, the COX-2 and mPGES-1 RNA levels are induced to within 2-fold of each other, 5.9 and 9.5 pmol mRNA/g total RNA, respectively.

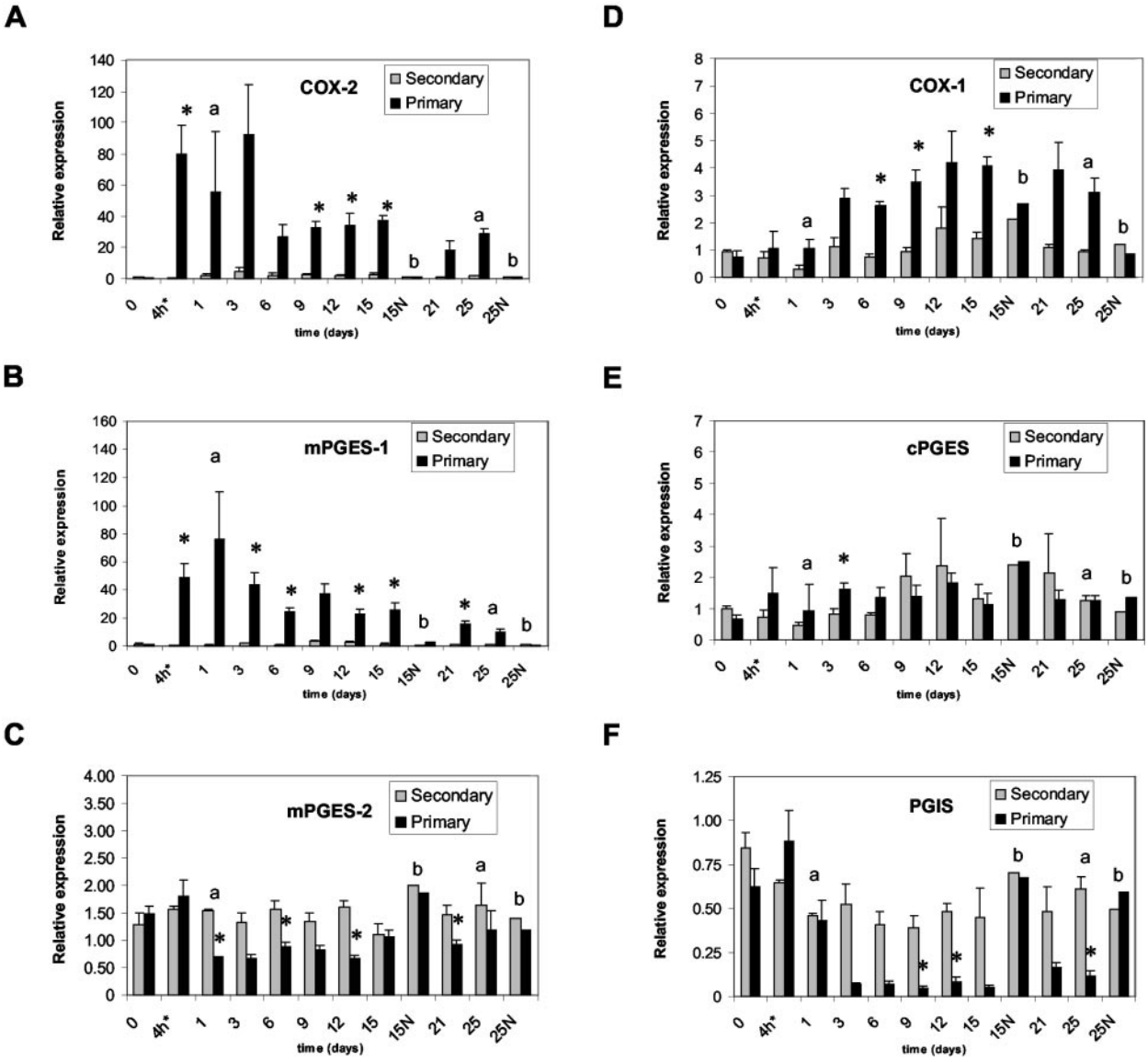

FIGURE 2. Real-time quantitative PCR analysis of mRNA expression of COX-1, COX-2, mPGES-1, mPGES-2, cPGES/p23, and PGIS during the development of AIA. Rats were injected with 0.5 mg *M. butyricum* in the right hind footpad (primary) and analyzed at the indicated time periods following adjuvant administration. Naive animals were also sacrificed at days 15 and 25, and are labeled as 15N and 25N. At the indicated time, animals were sacrificed and paws were collected. Total RNA was isolated, reverse transcribed, and analyzed by real-time quantitative PCR analysis. The levels of expression of COX-2 (*A*), mPGES-1 (*B*), mPGES-2 (*C*), COX-1 (*D*), cPGES/p23 (*E*), and PGIS (*F*) are expressed in mRNA quantity relative to that of the secondary paw at day 0, after normalization to 18S rRNA. Data are presented as the mean ± SEM of $n = 3$ rats, unless otherwise indicated (a, $n = 2$; b, $n = 1$). Statistical analysis shown was performed using a paired *t* test between the secondary and primary paw; ∗, designates $p < 0.05$. In addition, ANOVA analysis of the data is presented in *Materials and Methods*.

Induction of mPGES-1 protein in adjuvant-treated paws

Membrane and soluble fractions were prepared from the soft tissue of the adjuvant- and vehicle-treated rat paws. Proteins were electrophoresed on 4–20% SDS-PAGE gels, and analyzed for mPGES-1, COX-2, or COX-1 protein expression by immunoblot analysis with specific antisera for each protein (Figs. 4*A* and 5). In the absence of any adjuvant administration, mPGES-1 and COX-2 protein levels were close to the lower limit of detection with the antisera used. The induction of mPGES-1 was detected on day 1 and persisted to day 25 following adjuvant treatment in the primary paw. The maximum induction was measured at days 1–3 with a 60- to 80-fold increase of mPGES-1 as compared with the secondary paw at time zero (Fig. 5*A*). COX-2 protein induction was detected at all time points starting from day 1, with maximal induction of COX-2 measured at days 3 and 6. Constitutive levels of COX-1 protein were detected on day 0 in both the primary and secondary paws. A 2- to 4-fold increase of COX-1 was detected in the primary vs secondary paw during the time course of AIA (Fig. 5*C*).

The expression of cPGES/p23 protein was also analyzed in the corresponding supernatant fractions remaining from the membrane preparations analyzed for mPGES-1, COX-1, and COX-2 expression. In contrast to mPGES-1, constitutive levels of cPGES/p23 were detected in both primary and secondary paws (day 0, Fig. 4*B*). The levels of cPGES/p23 protein increased 2- to 6-fold following adjuvant treatment (Figs. 4*B* and 5*B*). The increase in protein expression for cPGES/p23 was similar to that of COX-1 and ~10- fold lower than that observed for mPGES-1 (Fig. 5).

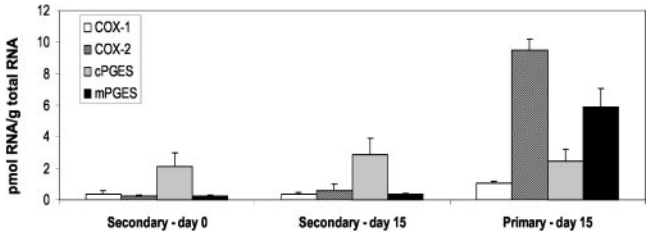

FIGURE 3. Quantitative determination of mPGES-1, COX-2, COX-1, and cPGES/p23 mRNA expression in AIA. Rats injected with 0.5 mg *M. butyricum* (primary) in the right hind footpad were analyzed at days 0 and 15. Total RNA was isolated and reverse transcribed, and real-time quantitative PCR analysis was performed. Quantification was performed using standard curves made from serial dilutions of known amounts of plasmids containing the cDNA of the genes of interest. Data are reported as the mean ± SEM of $n = 3$ rats.

Production of PGE_2 and PGI_2 in inflamed paws

The soluble extracts of paws from the AIA time course were also analyzed for PGE_2 and 6-keto-$PGF_{1\alpha}$ (a measure of PGI_2) content (Fig. 6). PGE_2 amounts were at the limit of detection at time zero, but reached a peak of 4 ng/mg protein at day 1 (>40-fold induction). The levels of PGE_2 remained elevated throughout the time course and decreased to ~1 ng/mg protein at day 25. By day 25, an increase in PGE_2 in the secondary paw, which is several fold above the vehicle control, was also detected. A 2.5- and 5.5-fold increase in prostacyclin was only detectable at the 4-h and 1-day time points, respectively, in the primary paw. In contrast to PGE_2, the increase in prostacylin was transient and returned to basal levels from days 3 to 25.

Induction of PGES activity and inhibitor sensitivity

The cytosolic and membrane fractions of both the primary and secondary paws on days 1 and 3 postadjuvant treatment were analyzed for PGES activity using exogenous PGH_2. The cytosolic and membrane fractions in the secondary paw and the cytosolic fraction of the primary paw contained very low, if any, PGES activity above nonenzymatic degradation of PGH_2 (Table II). In contrast, the membrane fractions of the primary paw on days 1 and 3 had a >4-fold increase in PGES activity above the activity measured in the secondary paw. This PGES activity was inhibited to at least 90% with MK-886 and with a potency (IC_{50} = 2.5 ± 0.4 μM ($n = 4$, day 1) and 2.4 ± 0.3 μM ($n = 3$, day 3)) that is comparable to that of the recombinant rat mPGES-1 (IC_{50} = 3.2 μM) (7). These data suggest that all of the increased PGES activity in adjuvant-treated rat paws is membrane associated and MK-886 inhibitable, which is consistent with a major role for mPGES-1 in this model. Although MK-886 shows a reasonable potency as an inhibitor of mPGES-1 in vitro in microsomal assays, its potency is affected by binding to serum proteins. For example, MK-886 is a potent inhibitor of FLAP in human polymorphonuclear leukocytes with an IC_{50} of 2.5 nM for the inhibition of leukotriene biosynthesis that is significantly shifted to an IC_{50} of 1.1 μM in human whole blood (23). This 440-fold protein shift precludes the use of MK-886 as an inhibitor of mPGES-1 for in vivo experiments.

Discussion

The rat AIA model is a rodent model of joint inflammation that has been used for the preclinical development of nonsteroidal anti-inflammatory drugs and COX-2 inhibitors. Selective COX-2 inhibitors reduce the pain and inflammation in AIA along with a corresponding decrease of PGE_2 in the inflamed paw in this model (24, 25). It has recently been shown that a selective COX-1 inhibitor that does not inhibit the inflammation in AIA also does not result in inhibition of PGE_2 in the paw (26). These results demonstrate that COX-2-mediated PGE_2 production is the major pathway of PG formation that causes pain and inflammation in the AIA model. With the discovery of several terminal PGES, including mPGES-1 (4), mPGES-2 (10), and cPGES/p23 (5), it has become intriguing to determine which of these synthases is involved in the formation of the proinflammatory PGE_2 in AIA.

We have demonstrated using quantitative PCR that mPGES-1 and COX-2 are both significantly induced at early time points and to the same relative extent in the AIA model. COX-1 and cPGES/p23 are only slightly increased in the AIA model, and the relative maximal increase is at least 10-fold lower than for either COX-2 or mPGES-1. Levels of mPGES-2 RNA are slightly decreased during the time course analyzed in the AIA model. Interestingly, constitutive levels of cPGES/p23 RNA are >8-fold above either COX-2 or mPGES-1 resting RNA levels. Prostacyclin has been shown to play a role in acute inflammation (22). No significant induction of PGIS is detected in AIA; in fact, a decrease in PGIS RNA is detected over the 25-day time course in the primary paw.

At the protein level, neither mPGES-1 nor COX-2 is detectable to any appreciable extent in the rat paw in the absence of any

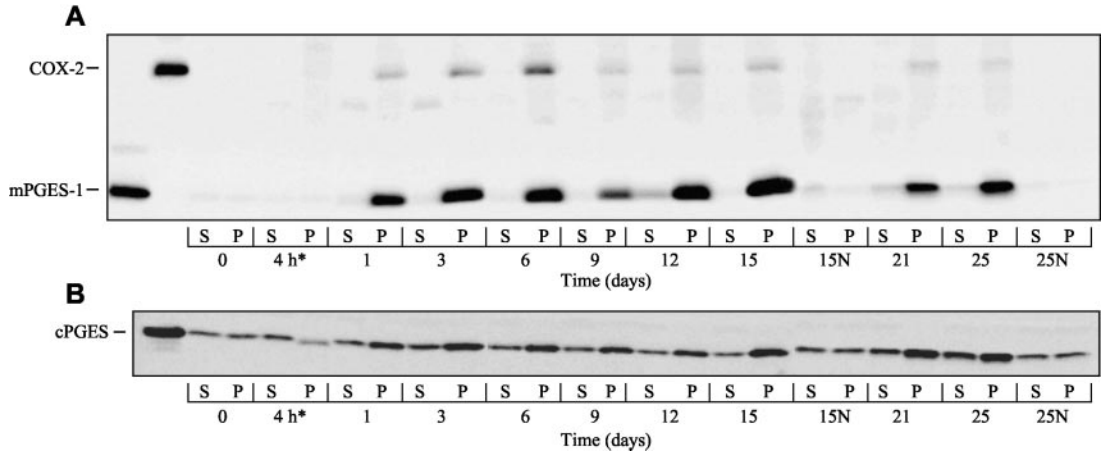

FIGURE 4. Immunoblot analyses of expression of mPGES-1, COX-2, and cPGES/p23 during the development of AIA in rats. Secondary (S) and primary (P) paws from adjuvant-treated and naive (N) rats were isolated. Equal amounts of protein were electrophoresed on 4–20% SDS-polyacrylamide gels, transferred electrophoretically to PVDF membrane, and analyzed by immunoblot using mPGES-1 and COX-2 polyclonal Abs (*A*) and a mAb raised to cPGES/p23 (*B*). Standards from mPGES-1, COX-2, and cPGES/p23 were obtained from recombinant expressed protein samples.

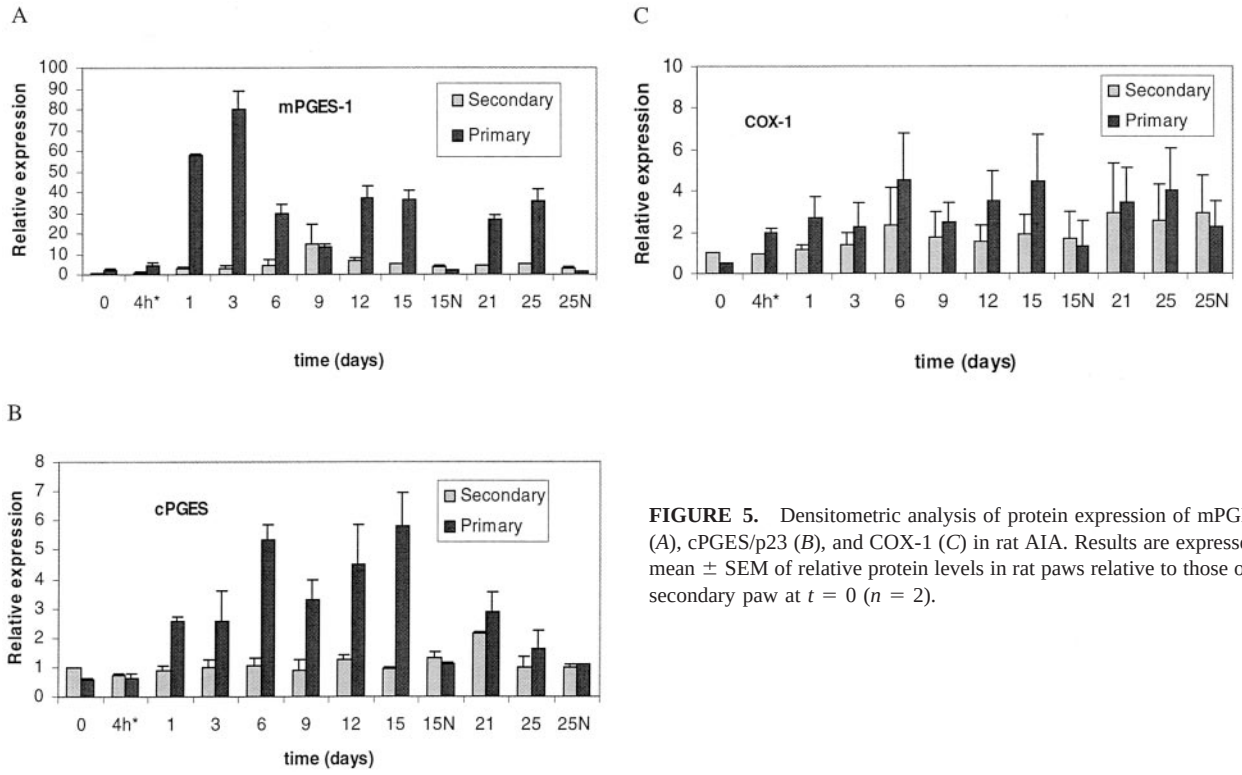

FIGURE 5. Densitometric analysis of protein expression of mPGES-1 (*A*), cPGES/p23 (*B*), and COX-1 (*C*) in rat AIA. Results are expressed as mean ± SEM of relative protein levels in rat paws relative to those of the secondary paw at $t = 0$ ($n = 2$).

inflammatory stimulus. This is in contrast to cPGES/p23, which is present in the nonadjuvant-treated paw. In the adjuvant-treated primary paw, mPGES-1 is coinduced with COX-2, with increased levels detected by 4 h and remained elevated for 15 days after administration of adjuvant. The pattern of induction observed by Taqman analysis is quite similar to the pattern of protein expression by immunoblot and suggests a reasonable correlation of elevated RNA and protein expression in the AIA model for mPGES-1. The cPGES/p23 enzyme was also slightly induced at the protein level between days 1 and 15, but the maximal induction was only 5- to 6-fold and is relatively low compared with the 70- to 80-fold induction of mPGES-1 in AIA. It is of interest that the increase in cPGES/p23 was also accompanied by a similar increase in COX-1 because these two enzymes have been suggested to preferentially couple for PGE_2 production. Measurement of PGES activity in the cytosolic and membrane fraction showed that only the membrane fraction contained any appreciable increase in PGES activity. The latter suggests that cPGES/p23, which is primarily expressed in cytosolic fractions, might not significantly contribute to PGE_2 synthesis at the site of inflammation in this model. Also, the PGES activity associated with the membrane fraction was inhibited by MK-886 ($IC_{50} = 2.4\ \mu M$) with a potency similar to that of the recombinant rat mPGES-1 enzyme ($IC_{50} = 3.2\ \mu M$) (7). These data suggest that the major PGES enzyme in the inflamed paws of the AIA model is mPGES-1.

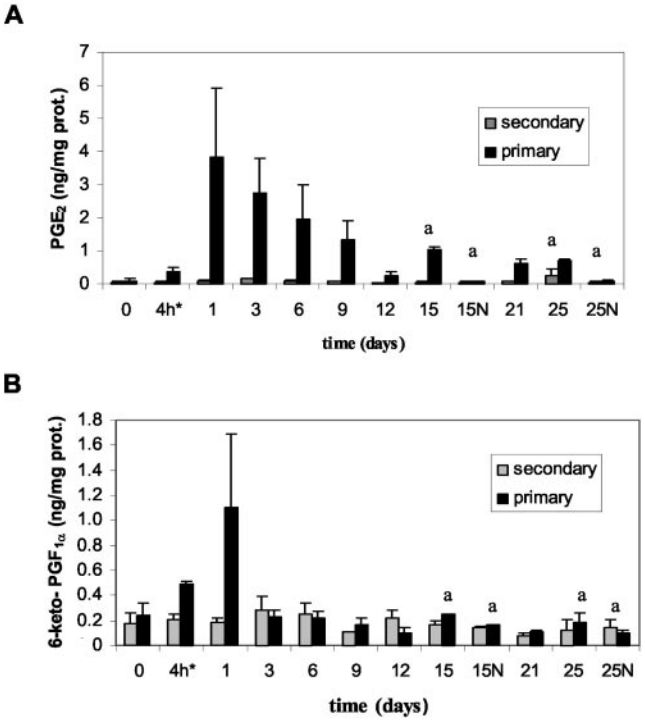

FIGURE 6. Measurement of PGE_2 and 6-keto-$PGF_{1\alpha}$ during the development of AIA. Soluble fractions of extracts prepared from the soft tissue of the rat paws were analyzed for levels of PGE_2 (*A*) and 6-keto-$PGF_{1\alpha}$ (*B*) by enzyme immunoassay. Data are presented as the mean ± SEM ($n = 3$ or a, $n = 2$).

Table II. *PGES activity in fractions from paws of AIA rats*[a]

Time	Paw Fraction	PGE_2 (ng/ml)	
		Primary paw	Secondary paw
Day 1	S100	32 ± 3 (4)	27 ± 6 (4)
	P100	138 ± 26 (4)	32 ± 1 (4)
Day 3	S100	27 ± 7 (4)	30 ± 6 (4)
	P100	152 ± 19 (3)	33 ± 3 (3)
Nonenzymatic		21 ± 4 (4)	

[a] Soluble (S100) and microsomal membrane fractions (P100) were prepared from pulverized rat paw tissue extracts and characterized for production of PGE_2. Protein samples (0.1 mg of protein/ml) were incubated with 1 μM PGH_2 for 40 s in 100 mM phosphate buffer, pH 7.4, 2 mM EDTA, and 2.5 mM GSH, and the reaction was terminated with 0.1 N HCl and 1 mg/ml stannous chloride. PGE_2 production was analyzed by immunoassay, and all results are reported as means ± SEM ($n = 3$ or 4).

To correlate the production of mediators of inflammation with the variations in the expression of terminal synthases, we also measured tissue levels of PGE_2 and PGI_2. The early induction of PGE_2 suggests a contribution of this mediator to the initial increase in paw edema measured over the first 6 days postadjuvant treatment. PGI_2 demonstrated an early initial spike, and this may suggest an acute role for PGI_2 and a more sustained chronic role in inflammation for PGE_2.

The AIA model has been demonstrated to contain an inflammatory component produced by COX-2-mediated PGE_2 production using a selective COX-2 inhibitor (24) and anti-PGE_2 Ab treatment (2). A recent report has also demonstrated mPGES-1 induction in brain endothelial cells and in the parenchyma of the paraventricular hypothalamic nucleus in the AIA model, suggesting a CNS component of PGE_2 that may be regulated by mPGES-1 (27). We have demonstrated a significant induction of mPGES-1 during the development of inflammation and increased PGE_2 production in the rat AIA, and the measurable activity in the treated primary paw is inhibitable by MK-886. These data suggest that mPGES-1 plays a significant role in joint inflammation in rat AIA, and that this model may be suitable for the evaluation of pharmacological agents that specifically inhibit mPGES-1.

References

1. Narumiya, S., Y. Sugimoto, and F. Ushikubi. 1999. Prostanoid receptors: structures, properties, and functions. *Physiol. Rev. 79:1193.*
2. Portanova, J. P., Y. Zhang, G. D. Anderson, S. D. Hauser, J. L. Masferrer, K. Seibert, S. A. Gregory, and P. C. Isakson. 1996. Selective neutralization of prostaglandin E_2 blocks inflammation, hyperalgesia, and interleukin 6 production in vivo. *J. Exp. Med. 184:883.*
3. FitzGerald, G. A., and C. Patrono. 2001. The coxibs, selective inhibitors of cyclooxygenase-2. *N. Engl. J. Med. 345:433.*
4. Jakobsson, P. J., S. Thoren, R. Morgenstern, and B. Samuelsson. 1999. Identification of human prostaglandin E synthase: a microsomal, glutathione-dependent, inducible enzyme, constituting a potential novel drug target. *Proc. Natl. Acad. Sci. USA 96:7220.*
5. Tanioka, T., Y. Nakatani, N. Semmyo, M. Murakami, and I. Kudo. 2000. Molecular identification of cytosolic prostaglandin E_2 synthase that is functionally coupled with cyclooxygenase-1 in immediate prostaglandin E_2 biosynthesis. *J. Biol. Chem. 275:32775.*
6. Murakami, M., H. Naraba, T. Tanioka, N. Semmyo, Y. Nakatani, F. Kojima, T. Ikeda, M. Fueki, A. Ueno, S. Oh, and I. Kudo. 2000. Regulation of prostaglandin E_2 biosynthesis by inducible membrane-associated prostaglandin E_2 synthase that acts in concert with cyclooxygenase-2. *J. Biol. Chem. 275:32783.*
7. Mancini, J. A., K. Blood, J. Guay, R. Gordon, D. Claveau, C. C. Chan, and D. Riendeau. 2001. Cloning, expression and up-regulation of inducible rat PGE synthase during LPS-induced pyresis and adjuvant induced arthritis. *J. Biol. Chem. 276:4469.*
8. Yamagata, K., K. Matsumura, W. Inoue, T. Shiraki, K. Suzuki, S. Yasuda, H. Sugiura, C. Cao, Y. Watanabe, and S. Kobayashi. 2001. Coexpression of microsomal-type prostaglandin E synthase with cyclooxygenase-2 in brain endothelial cells of rats during endotoxin-induced fever. *J. Neurosci. 21:2669.*
9. Beuckmann, C. T., K. Fujimori, Y. Urade, and O. Hayaishi. 2000. Identification of μ-class glutathione transferases M2-2 and M3-3 as cytosolic prostaglandin E synthases in the human brain. *Neurochem. Res. 25:733.*
10. Tanikawa, N., Y. Ohmiya, H. Ohkubo, K. Hashimoto, K. Kangawa, M. Kojima, S. Ito, and K. Watanabe. 2002. Identification and characterization of a novel type of membrane-associated prostaglandin E synthase. *Biochem. Biophys. Res. Commun. 291:884.*
11. Breyer, M. D., and R. M. Breyer. 2000. Prostaglandin E receptors and the kidney. *Am. J. Physiol. Renal Physiol. 279:F12.*
12. Guan, Y., Y. Zhang, A. Schneider, D. Riendeau, J. A. Mancini, L. Davis, M. Komhoff, R. M. Breyer, and M. D. Breyer. 2001. Urogenital distribution of a mouse membrane-associated prostaglandin E_2 synthase. *Am. J. Physiol. Renal Physiol. 281:F1173.*
13. Ek, M., D. Engblom, S. Saha, A. Blomqvist, P. J. Jakobsson, and A. Ericsson-Dahlstrand. 2001. Inflammatory response: pathway across the blood-brain barrier. *Nature 410:430.*
14. Chan, C. C., M. Panneton, A. M. Taylor, M. Therien, and I. W. Rodger. 1997. A selective inhibitor of cyclooxygenase-2 reverses endotoxin-induced pyretic responses in non-human primates. *Eur. J. Pharmacol. 327:221.*
15. Ushikubi, F., E. Segi, Y. Sugimoto, T. Murata, T. Matsuoka, T. Kobayashi, H. Hizaki, K. Tuboi, M. Katsuyama, A. Ichikawa, et al. 1998. Impaired febrile response in mice lacking the prostaglandin E receptor subtype EP3. *Nature 395: 281.*
16. Li, S., Y. Wang, K. Matsumura, L. R. Ballou, S. G. Morham, and C. M. Blatteis. 1999. The febrile response to lipopolysaccharide is blocked in cyclooxygenase-$2^{-/-}$, but not in cyclooxygenase-$1^{-/-}$ mice. *Brain Res. 825:86.*
17. Lazarus, M., B. K. Kubata, N. Eguchi, Y. Fujitani, Y. Urade, and O. Hayaishi. 2002. Biochemical characterization of mouse microsomal prostaglandin E synthase-1 and its colocalization with cyclooxygenase-2 in peritoneal macrophages. *Arch. Biochem. Biophys. 397:336.*
18. Uematsu, S., M. Matsumoto, K. Takeda, and S. Akira. 2002. Lipopolysaccharide-dependent prostaglandin E_2 production is regulated by the glutathione-dependent prostaglandin E_2 synthase gene induced by the Toll-like receptor 4/MyD88/NF-IL6 pathway. *J. Immunol. 168:5811.*
19. Mukherjee, A., V. G. Hale, O. Borga, and R. Stein. 1996. Predictability of the clinical potency of NSAIDs from the preclinical pharmacodynamics in rats. *Inflamm. Res. 45:531.*
20. Philippe, L., P. Gegout-Pottie, C. Guingamp, K. Bordji, B. Terlain, P. Netter, and P. Gillet. 1997. Relations between functional, inflammatory, and degenerative parameters during adjuvant arthritis in rats. *Am. J. Physiol. 273:R1550.*
21. Fletcher, D. S., W. R. Widmer, S. Luell, A. Christen, C. Orevillo, S. Shah, and D. Visco. 1998. Therapeutic administration of a selective inhibitor of nitric oxide synthase does not ameliorate the chronic inflammation and tissue damage associated with adjuvant-induced arthritis in rats. *J. Pharmacol. Exp. Ther. 284:714.*
22. Murata, T., F. Ushikubi, T. Matsuoka, M. Hirata, A. Yamasaki, Y. Sugimoto, A. Ichikawa, Y. Aze, T. Tanaka, N. Yoshida, et al. 1997. Altered pain perception and inflammatory response in mice lacking prostacyclin receptor. *Nature 388: 678.*
23. Gillard, J., A. W. Ford-Hutchinson, C. Chan, S. Charleson, D. Denis, A. Foster, R. Fortin, S. Leger, C. S. McFarlane, H. Morton, et al. 1989. L-663,536 (MK-886) (3-[1-(4-chlorobenzyl)-3-*t*-butyl-thio-5-isopropylindol-2-yl]-2,2-dimethylpropanoic acid), a novel, orally active leukotriene biosynthesis inhibitor. *Can. J. Physiol. Pharmacol. 67:456.*
24. Chan, C. C., S. Boyce, C. Brideau, S. Charleson, W. Cromlish, D. Ethier, J. Evans, A. W. Ford-Hutchinson, M. J. Forrest, J. Y. Gauthier, et al. 1999. Rofecoxib (Vioxx, MK-0966; 4-(4′-methylsulfonylphenyl)-3-phenyl-2-(5H)-furanone): a potent and orally active cyclooxygenase-2 inhibitor: pharmacological and biochemical profiles. *J. Pharmacol. Exp. Ther. 290:551.*
25. Anderson, G. D., S. D. Hauser, K. L. McGarity, M. E. Bremer, P. C. Isakson, and S. A. Gregory. 1996. Selective inhibition of cyclooxygenase (COX)-2 reverses inflammation and expression of COX-2 and interleukin 6 in rat adjuvant arthritis. *J. Clin. Invest. 97:2672.*
26. Ochi, T., and T. Goto. 2002. Differential effect of FR122047, a selective cyclooxygenase-1 inhibitor, in rat chronic models of arthritis. *Br. J. Pharmacol. 135: 782.*
27. Engblom, D., M. Ek, I. M. Andersson, S. Saha, M. Dahlstrom, P. J. Jakobsson, A. Ericsson-Dahlstrand, and A. Blomqvist. 2002. Induction of microsomal prostaglandin E synthase in the rat brain endothelium and parenchyma in adjuvant-induced arthritis. *J. Comp. Neurol. 452:205.*